

Water-inrush mechanism research mining above karst confined aquifer and applications in North China coalmines

Herong Gui^{1,2} · Xiaomei Song³ · Manli Lin^{1,2}

Received: 25 May 2016 / Accepted: 17 March 2017 / Published online: 6 April 2017
© Saudi Society for Geosciences 2017

Abstract Karst water poses great menace to vast and extensive coal-bearing region in China. The large water bodies which are highly pressurized have caused appalling disasters. This study takes example from the North China coal-bearing region and introduces karst aquifer distribution. It points out the major contributors to karst water burst and its relation with bottom plate deformation under mining activities. The analysis of criteria to determine karst water burst focuses on two elements (water burst coefficient and critical water burst index) and their positive application in Huaibei Luling coalmine, North China coal-bearing region. All achievements can be of reference to other coal-producing countries which are confronted with karst water hazards.

Keywords Karst water hazard · Bottom plate deformation · Water burst coefficient · Critical water burst index · China

Introduction

Globally, water hazard is one of the serious disasters in coalmines. Mine water hazards have led to a large number

of casualties and property losses. The water inrush accidents of Lofthouse Colliery mine, Northumberland of England, caused 10 deaths in 1973 and the water inrush of Chasnala Colliery mine, Jharia of India, killed 375 people in 1975 (Vutukuri and Singh 1995).

In China, the complex hydrogeological conditions are inherent with over 30 common types of water hazards (Gui and Lin 2016) in which the karst water hazard is more serious.

The coal areas threatened by limestone karst water hazards are over 60% of the total coal-bearing regions of China, amounting to over tens of billion tons of coal reservation. In particular, North and South China regions have suffered the most from karst water burst disasters. Such accidents struck more frequently and more deadly due to large volumes of highly pressurized water. On December 3rd, 1995 at Fengfeng Wutong coalmine in Henan, North China, a catastrophic Ordovician karst water accident flooded the pit and killed 17 people, recording instant water flow as high as 34,000 m³/h. On March 1st, 2010, in Shenhua Luotuoshan coalmine, Northwest region was struck by Ordovician karst water accident. The instant maximum water flow recorded at 60,036 m³/h, flooding the entire mine and leaving 32 dead people (Wu et al. 2013).

In efforts to meet the Chinese requirements, “high yield, high efficiency, safety” on coal production, the industry has invested enormously on research to understand karst water as a menace and the burst mechanism when mining over pressure-bearing karst aquifer. The achievements (Wu et al. 2009; Sui et al. 2011; Sun et al. 2015; Zeng et al. 2016) will be of relevance to other countries facing similar threats from karst water in coalmines.

✉ Herong Gui
guiherong@163.com

¹ School of Resources and Civil Engineering, Suzhou University, Suzhou, Anhui 234000, China

² National Engineering Research Center of Coal Mine Water Hazard Controlling, Suzhou, Anhui 234000, China

³ School of Earth and Engineering, Anhui University of Science and Technology, Huainan, Anhui 232001, China

Theory and methods

Distribution features of karst aquifer

Taking Huaibei coal field in North China, the exposed strata, from newly formed to old, are Quaternary, Neogene, Permian, Carboniferous, and Ordovician. Among the strata, Carboniferous Taiyuan formation and the top of Ordovician limestone contain pressure-bearing karst aquifer which are detrimental to coal mining (Fig. 1).

A	TM / m	SM / m	Pillar 1:5000	Lithological propertied
Q	235.2	235.2		Clay,sandy clay,fine sand,interbedded strata of silty clay Clay, sandy clay
N	252.0	16.8		Primarily sandy mudstone and siltstone,K7 sandstone at bottom
P _{2s}	316.7	64.8		Mustone,sandy mudstone
	363.9	47.1		Primarily sandy mudstone,intercalated with siltstone and siltstone
	464.7	100.8		K6 medium sandstone
	521.6	56.9		Primarily siltstone and sandy mudstone with thin coal seam (none-minable)
	642.7	121.1		Primarily mudstone and siltstone,with 6 layers of coal seam
P _{1x}	705.2	62.5		Shale interbedded with siltstone
	748.4	43.2		Primarily mudstone and siltstone, with coal seam 10(minable)
P _{1s}	795.7	47.2		The bottom aquifuge, upper & lower is mudstone,middle is fine sandstone & siltstone
	852.7	57.1		4limestone seams,of which L3 & L4 are thicker and even distributed
C _{3t}	913.5	60.8		Primarily mudstone and 1-2 strata of thin limestone
	950.1	36.6		5-6 strata of limestone,of which L8 and L10 are thicker and evenly distributed
	999.6	49.5		Bauxitic mudstone
C _{2b}	1011.2	11.6		Limestone,karst fissures developed with high water yield and high water pressure
O ₂	1081.1	699		Limestone,karst fissures developed with high water yield and high water pressure

Note : A—Stratigraphic age ;
 TM—Accumulative thicness /m ;
 SM—Strata thicness /m ;
 Q—Quaternary ; N—Neogene ;
 P_{2s}—Permian upper Shihezi formation ;
 P_{1x}—Permian lower Shihezi formation ;
 P_{1s}—Permian upper Shanxi formation ;
 C_{3t}—Carboniferous Taiyuan formation ;
 C_{2b}—Carboniferous Benxi formation ;
 O₂—Ordovician ;

Fig. 1 Strata bar graph of Huaibei coalfield, Anhui

Permian contains 20–30 strata of coal seams, concentrating in the top Permian upper Shihezi formation and lower Permian middle-level Shihezi formation and Shanxi formation. Specifically, the strata between the minable seam in lower Shanxi formation and the top limestone in Carboniferous Taiyuan formation are formed of mudstone, fine sandstone, and siltstone, which produce low water yield. The strata are generally referred to as coal seam bottom plate aquifuge (simplified as bottom aquifuge). The aquifuge is of 50–60 m thickness or as thick as 75 m.

Carboniferous Taiyuan formation, located under the bottom aquifuge, has a thickness range of 100–170 m with an average of 120 m. The formation comprises thin layers of limestone, mudstone, sandy mudstone, sandstone, and thin coal seam. There are a total of 10–14 layers of limestone (accumulative thickness f 50–75 m and an average of 64 m), which are named from top down as L₁, L₂, ..., L₁₄ limestone, the L₁ and L₂ are thinner (each of 5 m in thickness), and water-free. L₃ and L₄ are thicker (each of 12 m in thickness) and with evenly distributed water yield, which are the direct water source for water inrush in coalmining.

Based on the hydrogeological test to the aquifer of Taiyuan formation, the permeability coefficient *K* of L₁~L₄ limestone is 0.066~0.3512 m/day and the unit inflow *q* is 0.022~2.338 L/(s.m), from which we think that the limestone permeability and the water abundance of Taiyuan formation all are good.

Ordovician limestone, located under the limestone layers in Carboniferous Taiyuan formation, has a thickness over 500 m with development of karst fissures. Water pressure reaches as high as 5.0–7.5 MPa with high water yield. The permeability coefficient *K* is 1.34~1.98 m/day and the unit inflow *q* is 0.718~3.61 L/(s.m), which means that the Ordovician limestone is rich in water as very strong karstification and the permeation conditions of the groundwater of the limestone are very good. Ordovician karst water generates hydraulic connection with the limestone layers in Carboniferous Taiyuan formation and the Permian strata through water-conductive faults or karst collapse column, posing severe menace to mining safety.

Factors influencing karst water burst

In coal mining, triggers to karst water disasters are related to the following factors (Bieniawski 1995; Kwasniewski and Wang 1999; Zhang 2005; Sergio et al. 2009):

- (1) Thickness and strength of the bottom aquifuge. The thicker and harder the bottom aquifuge is, the stronger it is to resist water burst from the karst aquifer.

- (2) The growth level of pre-existing formation. The pre-existing formation, such as faults and fissures, will attenuate the strength of the bottom aquifuge. The thickness of the water-resisting aquifuge, or also named as “effective aquifuge thickness,” is smaller than the thickness of the original bottom aquifuge, thus giving rise to the possibility of water burst from the karst aquifer.
- (3) Water head pressure of karst aquifer. The karst aquifer is pressure-bearing. If the water head pressure rises, there is higher possibility of water burst accident.
- (4) Mining thickness and mining method. The further mining goes into the coal seam, the deeper the destruction to the bottom mining plate. Water burst is prone to happen if the effective aquifuge thickness of aquifuge shrinks. Backfill mining and room and pillar mining cause less destruction to the bottom aquifuge, thus lowering possibility of water burst from the karst aquifer.
- (5) Mine pressure. Areas with concentrated mine pressure are more susceptible to water burst.
- (6) Tectonic stress (including current and residual tectonic stress). Current tectonic stress releases in the form of earthquake, which will cause water burst if the seismic origin is close to coalmine and of greater magnitude. Residual tectonic stress tends to culminate in synclinal shaft and plunging folds as well as the junctures, where water burst is more probable to strike if evoked by other tectonic stress such as earthquake and mine pressure, etc. (Gui et al. 1999; Qiu et al. 2015).

Recorded karst water-incurred accidents in China coalmines have shown that water burst happens more dominantly during tunnel excavation and working face mining, where the former is more frequently stricken than the latter in statistics. In Hebei Jingjing coalmine, North China coal-bearing region, the ratio of tunnel excavation accidents to face mining accidents is 2.7:1 (Fang et al. 1987). The underlying reason is that tunnel excavation would hit many minor faults which would trigger water burst. Working panels, in contrast, are designed away from major faults. Minor faults during face mining would have been exposed in excavation of wind tunnels and machine tunnels. As a result, frequency of water burst in working face mining is much smaller than that in tunnel excavation (Bieniawski 1982; Zhang et al. 2014).

Bottom plate deformation and water burst

Rule of bottom formation: the “three bottom strata”

Mining activity breaks the original tectonic stress balance, which readjusts in a way to stretch or destruct the rock mass in the bottom aquifuge. Through field measurements and lab simulations of the bottom coal seam deformation, the bottom rock plate has shown the tendency to stratify under mining

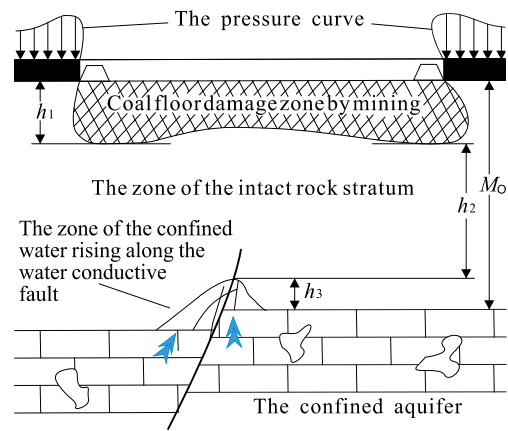


Fig. 2 Diagram of the “three bottom strata” in bottom aquifuge

forces just as the roof overlying rock. From top down, the strata are destructed stratum in mining bottom plate, intact rock stratum, and pre-existing confined water-conductive stratum (collectively named as “three bottom strata”) (Li et al. 1987; Lu and Wang 2015), as shown in Fig. 2. Specifically, the depth (h_1) of “destructed stratum in mining bottom plate” is in direct proportion to the length of the inclined working panel (L), empirical formula being $h_1 = 0.11 L + 1.86$ (coefficient $R = 0.9694$); the “intact rock stratum” (h_2) is the part in the bottom aquifuge which remains intact after mining with functional water resistance; the height of “pre-existing confined water-conductive stratum” (h_3) refers to the height rise of the karst pressurized water through the fissures or fault crushed zone in the bottom aquifuge. The discovery of the “three bottom strata” is of significance to the accurate evaluation of water resistance of bottom aquifuge and the analysis of water burst from karst aquifer (Gui et al. 2016).

- (1) Due to the presence of h_1 and h_3 , the effective aquifuge thickness in the bottom aquifuge equals to $h_2 = M_0 - (h_1 + h_3)$, while lowering the capability to resist water pressure

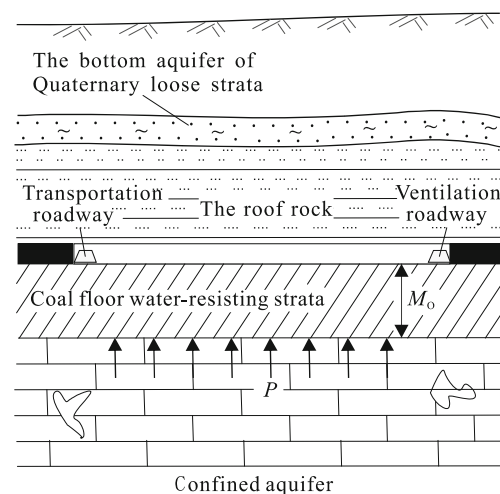


Fig. 3 Diagram of water burst coefficient

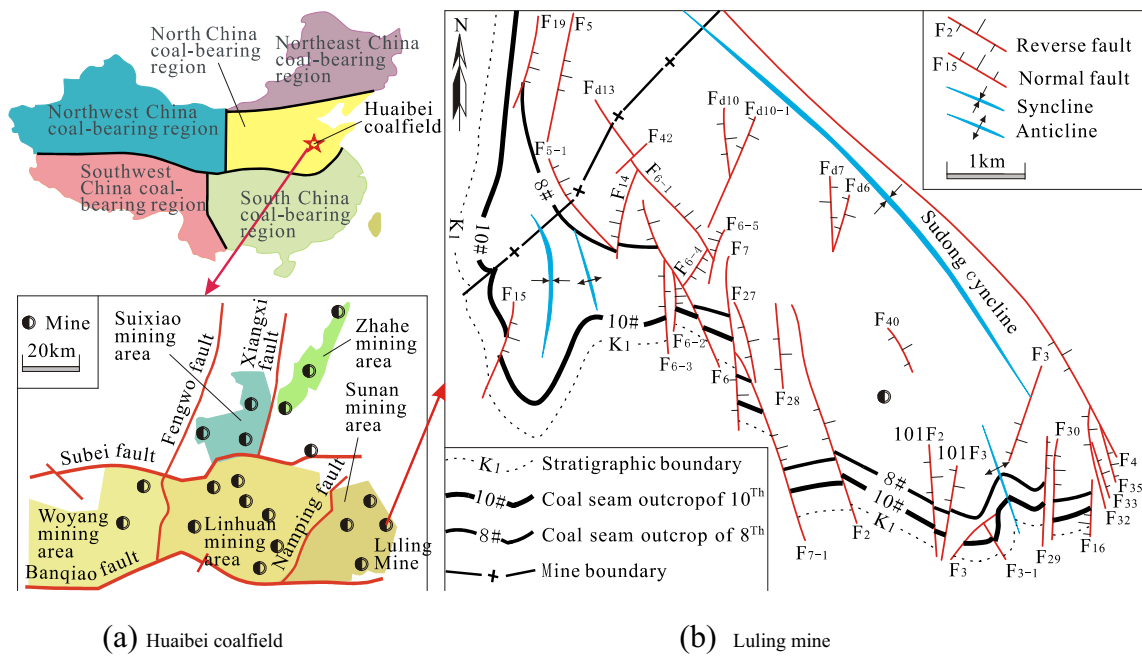


Fig. 4 Geological structure distribution of Luling mine (b) in Huaibei coalfield (a)

from karst aquifer. As a result, there is the risk of water burst.

- (2) If the faults in bottom plate are highly water-conductive, the pressurized karst water will rise higher (h_3) through faults or event channel with the destructed stratum in mining bottom plate (where h_2 diminishes to non-existent). Under such circumstance, water burst from karst aquifer is inevitable.

- (2) The height of the pre-existing confined water-conductive stratum (h_3) can be determined by measuring dynamic water pressure and volume using hydraulic fracturing method (Hayashi et al. 1997). In addition, h_3 can also be obtained through simulation tests of similar materials and numerical simulation (Yin and Hu 2008; Wang 2015).
- (3) The thickness of the intact rock stratum is as follows: $h_2 = M_0 - (h_1 + h_3)$.

Measuring the height of the “three bottom strata”

- (1) The depth of the destructed stratum in mining bottom plate (h_1) can be measured by water infusion into the bottom aquifuge (Jiang 2009) or by numerical simulation of hydraulic fracturing based on the functional relation between the permeability coefficient of bottom rock and damage variables (Gidley et al. 1989; Murdoch and Slack 2002; Xie et al. 2009) or by FLAC^{3D} numerical simulation (Wu et al. 2008; Zheng et al. 2015).

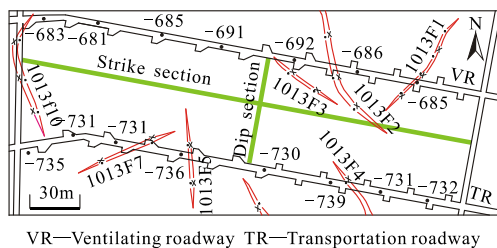


Fig. 5 The geological model of the simulation calculation of No. 1013 working face in Luling coalmine

Water burst evaluation index in karst aquifer

Water burst coefficient (T_s)

By the mid-1960s, in order to prevent water burst from karst aquifer and meet the evaluation needs of bottom plate safety, the coal industry in China proposed the concept of bottom plate “water burst coefficient” (T_s) (Wang and Park 2003), which represents the maximum hydrostatic pressure bearable to per 1-m-thick bottom aquifuge (Fig. 3). The formula is as follows:

$$T_s = \frac{P}{M_0} \tag{1}$$

In the formula, M_0 is the thickness of bottom aquifuge (m); P is the hydraulic pressure in karst aquifer exerted on the bottom aquifuge (MPa).

As is stipulated in the “National protocols for coalmine water hazards control” (SACMS 2009), when bottom

Table 1 The physical and mechanical parameters of rock and coal

Rock or coal	Density $\rho/\text{kg/m}^3$	Bulk modulus G/MPa	Shear modulus K/MPa	Tensile strength R_t/MPa	Cohesion C/MPa	Internal friction angle $\varphi/^\circ$
Medium sandstone	2375	10,800	1600	2	11	50
Coal	1270	5600	4170	1.2	1.2	38
Siltstone	2000	2300	1000	2.3	18	40
Sandy mudstone	2436	4500	1600	2.3	25	30
Mudstone	1600	100	70	2.5	12	25

aquifuge is destructed by faults and other geological structure, T_s shall be no bigger than 0.06 MPa/m; when there is no such destruction, T_s shall be no bigger than 0.1 MPa/m.

Due to mining activities, the bottom plate can be destructed in a way that pressurized karst water rises through pre-existing structure (such as faults and fissures), diminishing the effective aquifuge thickness. As a result, formula (1) turns into the following:

$$T_s = \frac{P}{h_2} = \frac{P}{M_0 - (h_1 + h_3)} \tag{2}$$

When the fissures and faults are not existent in bottom aquifuge, there is no “pre-existing confined water-conductive stratum” (i.e., $h_3 = 0$), generating $T_s = P/(M_0 - h_1)$.

Critical water burst indicator (I)

Water burst from karst aquifer is caused jointly by mining pressure and hydraulic pressure in karst aquifer, as well as a manifestation of “rock-water-stress” coupling effect. Therefore, the relation between rock (rock mass in bottom aquifuge), water (pressurized water in karst aquifer), and stress (mine pressure and tectonic stress) can be utilized as the indicator for water burst from karst aquifer (Dong 2010).

$$I = \frac{P}{\sigma_3} \tag{3}$$

Table 2 The physical and mechanical parameters of joint surfaces

Rock or coal	Normal stiffness j_{kn}/GPa	Shear stiffness j_{ks}/GPa	Cohesion j_{co}/MPa	Internal friction angle $j_{fr}/^\circ$	Tensile strength j_{ten}/MPa
Medium sandstone	5	2.8	3.5	17	0.22
Coal	0.9	0.8	0.6	7	0.1
Siltstone	5	2.8	7	17	0.22
Sandy mudstone	8.6	4.7	3.5	11	0.3

In the formula, I is the critical indicator of water burst (when $I < 1.0$, water burst is unlikely to happen; when $I > 1.0$, water burst is very likely to happen; P is the karst water pressure (MPa) on the rock mass in the bottom aquifuge; σ_3 is the minimum main horizontal stress (MPa) on the rock mass in the bottom aquifuge.

Water-resistance coefficient (Z)

To apply hydraulic fracturing on bottom aquifuge through drilling a number of holes in the mining field (Liu et al. 2007), the water-resistance coefficient is as follows:

$$Z = \frac{P_f}{R} \tag{4}$$

In the formula, P_f is the pressure value (MPa) that fractures rock mass in the bottom aquifuge, $P_f = 3\sigma_3 - \sigma_1 + \sigma_\tau - P_0$; σ_1 and σ_3 correspond to the maximum and minimum main horizontal stress on bottom aquifuge rock; σ_τ refers to the tensile strength (MPa) of the bottom rock plate; P_0 is the pore water pressure (MPa) in the bottom rock plate; R is the extension radius (m) of the fissures, usually at 40–50 m.

- (1) Water burst will not happen if the fracture pressure to bottom rock plate (P_f) is bigger than karst water pressure (P);
- (2) When the fracture pressure to bottom rock plate (P_f) is smaller than karst water pressure (P), comparing to the total water-resistance of effective aquifuge $Z_T (Z_T = Z h_2)$,

if $Z_T > P$, water burst will not happen; otherwise, there is the risk of water burst (Huang and Li 2008).

In recent years, there are other indicators, such as fragility index (Wu et al. 2007) and coupling geographic information system (GIS) with artificial neural network (ANN) (Wu et al. 2006), etc., in addition, to the above three individual index for the evaluation of water burst from karst aquifer in China coalmines.

Application and discussion

Due to space limit, this article here only introduces application of two commonly seen indicators (water burst coefficient and critical indicator of water burst) in Luling coalmine.

Luling coalmine is located in the Sunan mining area of Huaibei coalfield. From the view of the regional structure (Fig. 4a), there are two E-W orientation faults which are Banqiao fault and Subei fault and one nearly S-N orientation fault which is Nanping fault, respectively, developing in the southern, northern, and western of Luling coalmine. Fault structure is very well developed in Luling mine. In general, there are three sets of faults with NNW, NNE, SN orientations (Fig. 4b). It is clear that there are 45 faults with the throw greater than 10 m (19 normal faults and 26 reverse faults), 10 large faults with the throw greater than 100 m, 12 medium-sized faults with the throw between 30 and 100 m in the mine.

Application of T_s

To conduct water burst probability evaluation in the III horizontal of Huaibei Luling coalmine, Anhui of North China coal-bearing region, the horizontal (-590~900 m) 10[#] coal seam was under the threat of pressurized karst water in the limestone of Carboniferous Taiyuan formation.

- (1) About M_0 . Prospecting data revealed that the aquifuge thickness in the bottom plate was $M_0 = 56\sim 72$ m. As the L_1 and L_2 limestone strata in Carboniferous Taiyuan formation were thin with low water yield, grouting was conducted to the $L_1\sim L_2$ limestone strata to increase aquifuge thickness (ΔM) by 23 m on average.
- (2) About h_1 . The discrete element method (DEM) method is usually used for simulating the plastic failure of rock due to mining when there are discontinuous interfaces such as faults, joints, or levels of the strata in geological body. The discontinuous rock mass is considered to be composed of discrete rock blocks and discontinuous surfaces (fault planes, joint surfaces, or strata levels) during calculating by DEM method, while the rock blocks can move, rotate, or shape freely and the discontinuous surfaces can be compressed or separated.

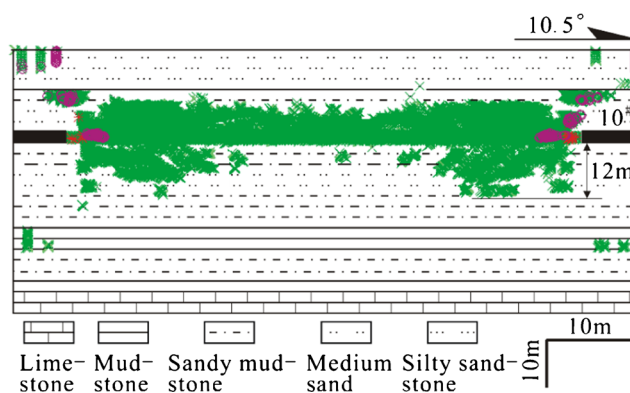


Fig. 6 Distribution of plastic failure zone on the tendency section of 1013 working face

By using the Universal Distinct Element Code (UDEC), the DEM can be used for the deformation and failure calculation of the discontinuous rock mass, while the failure criterion of the rock block is Mohr-Coulomb criterion, and the failure criterion of joints is the Mohr-Coulomb criterion of the joint slip surfaces.

The authors took the 1013 working face of No. 10 coal seam of the III horizontal in Luling coalmine as the geological model (Fig. 5), and, respectively, established trend model and tendency model of numerical calculation DEM according to the occurrence state of the rock strata shown in Fig. 1.

The average thickness of No. 10 coal seam is 2 m. The strata underneath the No. 10 coal seam are successively sandy mudstone, medium sandstone, sandy mudstone, and mudstone, accumulated thickness of which is 56~72 m. The strata above the No. 10 coal seam are successively sandstone, mudstone, siltstone, and sandstone, accumulated thickness of which is 38 m.

The physical and mechanical parameters of surrounding rock and coal in the model are shown in Table 1; the physical and mechanical parameters of the discontinuity surfaces (joint surfaces) are shown in Table 2.

The initial equilibrium of the model was carried out; then, the displacements were changed to zeros, while the DEM

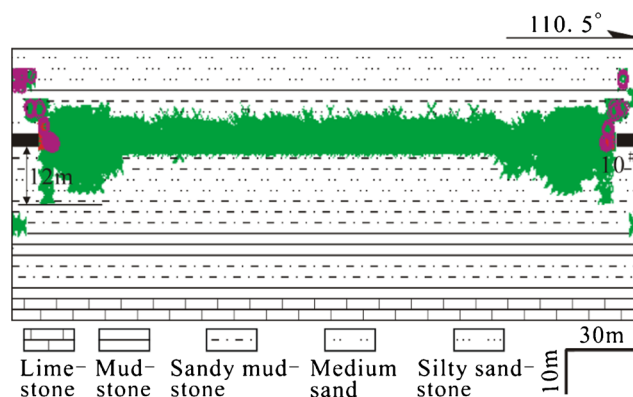


Fig. 7 Distribution of plastic failure zone on the strike section of 1013 working face

Table 3 Water burst coefficient in Taiyuan formation L_3 limestone stratum, Luling coalmine III horizontal

L_3 limestone water level/m	Mining elevation/m	Water head pressure P /MPa	Effective aquifuge thickness h_2 /m	Water burst coefficient T_s
-60	-590	5.30	67	0.08
-60	-900	8.40	83	0.10

calculation was conducted as the coal seam mining. The results of the DEM calculation are shown in Figs. 6 and 7, which we could see that there was one continuous plastic failure zone with 2 m depth and two plastic failure zones (each with the depth of 12 m) under the coal pillar on both sides of the 1013 working face. Besides, there were sporadic distribution fractures with the depth between 14 and 18 m. Therefore, the floor failure depth (h_1) of the No. 10 coal seam was determined to be 12 m.

- (3) About h_2 . The height rise of pressurized karst water caused by faults and fissures in bottom aquifuge was not considered in this case ($h_3 = 0$). So, the effective aquifuge thickness was $h_2 = M_0 + \Delta M - h_1 = (56 + 23 - 12) \sim (72 + 23 - 12) = 71 \sim 87$ m.
- (4) About P . The water level in Taiyuan formation L_3 limestone stratum was -60 m. The water head (P) pressure exerted on the bottom aquifuge (after grouting the $L_1 \sim L_2$ limestone strata) was 5.3~8.4 MPa.

Combing the above results, the water coefficient is shown in Table 3 based on formula (2).

It is thus clear that, if faults and fissures are not existent in bottom aquifuge, the water burst coefficients (T_s) are smaller than the standards in the “Chinese protocols for coalmine water hazards control” (i.e., $T_s \leq 0.1$). Mining safety is therefore guaranteed.

Application of I

Based on formula (3), to obtain tectonic stress values using acoustic emission (AE) method (Liu and Liu 2012; Xu et al. 2015) on Luling coalmine III horizontal, with the minimum main stress value (σ_3), the critical indicator (I) of water burst can be determined as in Table 4.

The spots where critical water burst indicator was over 1, located west to the III horizontal mechanic tunnel, with a value of 3.23 are exposed to higher risks of water burst from karst aquifer. The other two spots where $I < 1.0$ are safer from water burst.

The evaluation results using water burst coefficient and critical water burst indicators can be of reference to which measures shall be taken to prevent water burst from karst aquifer, especially the areas where the critical water burst indicator is over 1 (III horizontal mechanic tunnel west). Further prospecting into bottom aquifuge structure shall be carried out to identify abnormality in areas where water hazards are imminent. Built on the prospecting results, countermeasures such as draining karst aquifer or grouting bottom aquifuge (Xu et al. 2014) can be taken to contain T_s and I values within safety range before mining. In fact, Luling coalmine was not struck by karst water burst since its operation. This is to testify that evaluation based on water burst coefficient and critical water burst indicator is reliable in predicting risks of water burst from karst aquifer.

Table 4 Test values of tectonic stress using AE method in Luling coalmine III horizontal

Sites	Elevation/m	Depth/m	Max. main horizontal stress σ_1 /MPa	Min. horizontal stress σ_3 /MPa	Max. stress direction/ $^\circ$	Water pressure P /MPa	Critical water burst indicator I
III horizontal west-wing downhill return airway	-590	615	30.26	16.56	64.4	5.3	0.32
III horizontal mechanic tunnel east	-950	975	20.95	13.60	62.0	8.4	0.62
III horizontal mechanic tunnel west	-950	975	32.68	2.60	71.5	8.4	3.23

Conclusions

The following conclusions can be drawn based on the above analysis:

- (1) The comparative development of karst aquifer in China coal-bearing regions. Taking North China region, the karst aquifer threatening the lower Permian coal seam is composed of limestone strata in Carboniferous Taiyuan formation and Ordovician limestone strata, which form the major water source under the influence of water-conductive faults or karst collapse column.
- (2) With mining activity, water burst from karst aquifer is dependent on multiple factors, including the thickness and strength of the bottom aquifuge, development status of pre-existing structure, water pressure in karst aquifer, mine pressure, tectonic stress, mining depth, and mining method, etc.
- (3) With mining activity, there are three strata as a result of rock deformation in the bottom aquifuge, which from top down are destructed stratum in mining bottom plate (h_1), intact rock stratum (h_2), and pre-existing confined water-conductive stratum (h_3). The presence of h_1 and h_3 will diminish the effective thickness of bottom aquifuge, thus promoting risks of water burst from karst aquifer.
- (4) For China coalmines, there are a set of indicators to evaluate water burst risks from pressure-bearing karst aquifer, including water burst coefficient (T_s), critical water burst indicator (I), water-resistance coefficient (Z), etc. The two commonly used indicators (T_s , I) have demonstrated ideal results in Huaibei Luling coalmine, North China coal-bearing region.

Acknowledgement This article is funded by the National Natural Science Foundation of China (41373095), University Natural Science Research Project of Anhui Province (KJ2017A445) and Anhui Science and Technology Breakthrough Project (1501zc04048).

References

Bieniawski ZT (1982) Improved design of coal pillars for US mining conditions. In: proceedings of the first international conference on stability in underground mining, Vancouver, Canada, pp.16–18

Bieniawski ZT (1995) Design of mine pillars for long-term stability. In: proceedings of the international high-tech conference on geoenvironment, national mining university of Beijing, China, 245–257 pp

Dong SN (2010) Integrated in-stu tests for water inrush possibility evaluation in coal seam floors. *J Eng Geol* 18(1):116–119

Fang PX, Wei ZD, Liao ZS (1987) Special hydrogeology. Geological Publishing House, Wuhan, pp 261–263

Guidley JL, Holditch SA, Nierode DE (1989) Recent advances in hydraulic fracture. Society petroleum engineering monograph, 119–204 pp

Gui HR, Gong QN, Sun BK (1999) Study of control theory on water inrush from bed bottom in deep mining-basic study thinking and plan. *Journal of Huainan Institute of Technology* 19(4):1–4

Gui HR, Lin ML (2016) Types of water hazards in China coalmines and regional characteristics. *Nat Hazards* 84(2):1501–1512

Gui HR, Lin ML, Song XM (2016) Technical research on controlling major karst water hazards in China coalmine. *Water Practice and technology* 11(3):661–671

Hayashi K, Sato A, Ito T (1997) In-site stress measurement by hydraulic fracturing for a rock mass with many planes of weakness. *Int J Rock Mech Min Sci* 34(1):45–48

Huang H, Li C (2008) Forecast method of water inrush of floor over confined water body and its prevention and control measures. *Metal Mine* 6:126–129

Jiang Q (2009) Coal floor strata failure depth test of working face at big mining depth. *Coal Geology & Exploration* 37(4):30–33

Kwasniewski M, Wang JA (1999) 3-D numerical modeling and study of mine tremors associated with coal mining in the vicinity of major faults. *Publs Inst Geophys POL ACAD SC M-22(310):351–364*

Li BY, Shen GH, Jing ZG et al. (1987) Theory and practice to prevent water inrush in floor coal seam in mining panels. Conference proceeding of the 22nd international conference of mining safety, China coal industry publishing home, Beijing, 65–70 pp

Liu QM, Li WP, Ji ZK, Cheng W, Zeng XG, Jiao YL (2007) The method of actual measurement coefficient of water-resisting to evaluate dangerousness of Ordovician limestone water invasion. *Coal Geology & Exploration* 35(4):38–41

Liu QS, Liu KD (2012) Characteristics of in-situ stress field for deep levels in Huainan coalmine. *Rock Soil Mech* 33(7):2089–2096

Lu YL, Wang LG (2015) Numerical simulation of mining-induced fracture evolution and water flow in coal seam floor above a confined aquifer. *Comput Geotech* 67:157–171

Murdoch LC, Slack WW (2002) Forms of hydraulic fractures in shallow fine-grained formation. *J Geotech Geoenviron* 128(6):479–487

Qiu M, Shi LQ, Teng C, Xing TJ, Yu F (2015) Evaluation of water inrush risk for no.10 coal seam floor of Zhaoguan mine field. *Coal Geology & Exploration* 43(3):61–65

SACMS(State Administration of Coal Mine Safety) (2009) Regulations on coalmine water control. China Coal Industry Publishing Home, Beijing 83 pp

Sergio MR, Miguel RR, Francisco M et al (2009) Analysis of groundwater mining in two carbonate aquifers in sierra de Estepa (SE Spain) based on hydrodynamic and hydrochemical data. *Hydrogeol J* 17: 1617–1627

Sui WH, Liu JY, Yang SG et al (2011) Hydrogeological analysis and salvage of a deep coalmine after a groundwater inrush. *Environmental Earth Sciences* 62(4):735–749

Sun WJ, Wu Q, Liu HL et al (2015) Prediction and assessment of the disturbances of the coal mining in Kailuan to karst groundwater system. *Phys Chem Earth* 89-90:136–144

Vutukuri VS, Singh RN (1995) Mine inundation-case histories. *Mine Water and the Engineering* 14(9):107–130

Wang MJ (2015) In-site measurement and physical analogue on water inrush from coal floor induced by progressive intrusion of artesian water into protective aquiclude. *Chinese Journal of Geotechnical Engineering* 21(5):546–549

Wang JA, Park HD (2003) Coal mining above a confined aquifer. *Int J Rock Mech Min Sci* 40(4):537–551

Wu Q, Pang W, Dai YC, Yu J (2006) Vulnerability forecasting model based on coupling technique of GIS and ANN in floor groundwater bursting. *J China Coal Soc* 31(3):314–319

Wu Q, Xu H, Zhou WF (2008) Development of a 3D GIS and its application to karst areas. *Environ Geol* 54(5):1037–1045

Wu Q, Zhang ZL, Zhang SY, Ma JF (2007) A new practical methodology of the coal floor water bursting evaluating II: the vulnerable index method. *J China Coal Soc* 32(11):1122–1126

- Wu Q, Zhao SQ, Dong SN et al (2013) Handbook to coalmine water control. China Coal Industry Publishing Home, Beijing, pp 28–40
- Wu Q, Zhou WF, Pan GY et al (2009) Application of a discrete-continuum model to karst aquifers in North China. *Groundwater* 47(3):453–461
- Xie XH, Su BY, Gao XF, Duan XB (2009) Numerical study on water inrush above a confined aquifer in coal mining using hydro-fracturing. *Chin J Rock Mech Eng* 24(6):987–993
- Xu YC, Li JH, Liu BZ (2014) Reinforcement of working face by grouting in floor in Jiaozuo coal mining area. *Coal Geology & Exploration* 42(4):50–54
- Xu FT, Xie L, Zhang NH, Zhang HW (2015) Studies on acoustic emission characteristics of sandstone under uniaxial compression. *China Mining Magazine* 24(6):147–150
- Yin SX, Hu WY (2008) Rocks' water-resistance ability and natural progressive intrusion height. *Coal Geology & Exploration* 36(1):35–40
- Zeng YF, Wu Q, Liu SQ et al (2016) Vulnerability assessment of water bursting from Ordovician limestone into coal mines of China. *Environmental Earth Sciences* 75(22):1431 (1–11)
- Zhang JC (2005) Investigation of water inrush from aquifers under coal seams. *Int J Rock Mech Min Sci* 42(3):350–360
- Zhang R, Jiang ZQ, Zhou HY et al (2014) Groundwater outbursts from faults above a confined aquifer in the coalmining. *Nat Hazards* 71(3):1861–1872
- Zheng F, Wang LB, Zhu QX et al (2015) Simulation research on failure depth and stress distribution of coal seam floor based on FLAC^{3D}. *Coal. Technology* 34(2):106–108